Int J Appl Earth Obs Geoinformation 69 (2018) 133–147

Contents lists available at ScienceDirect

Int J Appl Earth Obs Geoinformation

journal homepage: www.elsevier.com/locate/jag

Mapping croplands, cropping patterns, and crop types using MODIS time-series data

Yaoliang Chen[a,b,c], Dengsheng Lu[a,c,*], Emilio Moran[c], Mateus Batistella[d,f], Luciano Vieira Dutra[e], Ieda Del'Arco Sanches[e], Ramon Felipe Bicudo da Silva[f], Jingfeng Huang[b], Alfredo José Barreto Luiz[d], Maria Antonia Falcão de Oliveira[e]

[a] State Key Laboratory of Subtropical Silviculture, School of Environmental & Resource Sciences, Zhejiang Agriculture and Forestry University, Hangzhou 311300, China
[b] Institute of Applied Remote Sensing & Information Technology, College of Environmental and Resource Sciences, Zhejiang University, China
[c] Center for Global Change and Earth Observations, Michigan State University, USA
[d] Brazilian Agricultural Research Corporation (Embrapa), Brasília, Brazil
[e] National Institute for Space Research, São Jose dos Campos, SP, Brazil
[f] Center for Environmental Studies and Research, State University of Campinas, Brazil

ARTICLE INFO

Keywords:
Croplands
Cropping patterns
Crop types
MODIS NDVI
Decision tree classifier
Brazil

ABSTRACT

The importance of mapping regional and global cropland distribution in timely ways has been recognized, but separation of crop types and multiple cropping patterns is challenging due to their spectral similarity. This study developed a new approach to identify crop types (including soy, cotton and maize) and cropping patterns (Soy-Maize, Soy-Cotton, Soy-Pasture, Soy-Fallow, Fallow-Cotton and Single crop) in the state of Mato Grosso, Brazil. The Moderate Resolution Imaging Spectroradiometer (MODIS) normalized difference vegetation index (NDVI) time series data for 2015 and 2016 and field survey data were used in this research. The major steps of this proposed approach include: (1) reconstructing NDVI time series data by removing the cloud-contaminated pixels using the temporal interpolation algorithm, (2) identifying the best periods and developing temporal indices and phenological parameters to distinguish croplands from other land cover types, and (3) developing crop temporal indices to extract cropping patterns using NDVI time-series data and group cropping patterns into crop types. Decision tree classifier was used to map cropping patterns based on these temporal indices. Croplands from Landsat imagery in 2016, cropping pattern samples from field survey in 2016, and the planted area of crop types in 2015 were used for accuracy assessment. Overall accuracies of approximately 90%, 73% and 86%, respectively were obtained for croplands, cropping patterns, and crop types. The adjusted coefficients of determination of total crop, soy, maize, and cotton areas with corresponding statistical areas were 0.94, 0.94, 0.88 and 0.88, respectively. This research indicates that the proposed approach is promising for mapping large-scale croplands, their cropping patterns and crop types.

1. Introduction

Agricultural production in Brazil has grown rapidly over the past three decades due to rising global demand, favorable commodity prices, and technological advances (Cohn et al., 2016; Dias et al., 2016). The improvement in crop management practices and cropland expansion and intensification have made Brazil the leading exporter in soybeans, sugar, meat, coffee, and orange juice (FAO, 2015). These advances require updating crop distribution information and its dynamic change in a timely way. In the past decade, much research on mapping cropland distribution in Brazil has been conducted (Arvor et al., 2011; Arvor et al., 2012; Brown et al., 2013; Epiphanio et al., 2010; Gusso et al., 2014; Rudorff et al., 2010; Victoria et al., 2012; Zhu et al., 2016). Landsat imagery has been extensively used for crop mapping due to its long-term historical records at no cost and relatively fine spatial resolution (Maxwell et al., 2004; Odenweller, 1984; Vieira et al., 2012; Zheng et al., 2015; Zhong et al., 2014). However, the revisiting times (16 days) result in difficulty collecting cloud-free images, especially in

* Corresponding author at: State Key Laboratory of Subtropical Silviculture, School of Environmental & Resource Sciences, Zhejiang Agriculture and Forestry University, Hangzhou 311300, China.
E-mail addresses: chengis0115@gmail.com (Y. Chen), luds@zafu.edu.cn, ludengsh@msu.edu (D. Lu), moranef@msu.edu (E. Moran), mateus.batistella@embrapa.br (M. Batistella), dutra@dpi.inpe.br (L.V. Dutra), ieda.sanches@inpe.br (I.D. Sanches), ramonbicudo@gmail.com (R.F.B. da Silva), hjf@zju.edu.cn (J. Huang), alfredo.luiz@embrapa.br (A.J.B. Luiz), marian.florestal@gmail.com (M.A.F. de Oliveira).

https://doi.org/10.1016/j.jag.2018.03.005
Received 23 November 2017; Received in revised form 11 March 2018; Accepted 12 March 2018
Available online 20 March 2018
0303-2434/

Table 1
Summary of selected approaches for mapping large-scale cropland distribution.

	Method	Description of examples	Key references
Pixel-based approaches	Traditional classifiers and machine learning classifiers	(1) Maximum likelihood classifier based on MODIS EVI time-series data to map crop types and cropping system in Mato Grosso, Brazil	Arvor et al. (2011)
		(2) Spectral angle mapper based on MODIS EVI time-series to map crop types in Paraná, Brazil	Grzegozewski et al. (2016)
		(3) Decision tree classifier based on MODIS NDVI and EVI time-series data to classify agricultural land use data in Mato Grosso, Brazil; based on MODIS NDVI time-series data to identify crop types in Kansas, USA or the conterminous USA; and based on LSWI, EVI, and NDVI time-series data to identify paddy rice in the southern China	Brown et al. (2013), Wardlow and Egbert (2010), Massey et al. (2017), Xiao et al. (2005)
		(4) Neutral network based on MODIS NDVI time-series data to classify crop types across Laurentian Great Lakes Basin, USA	Lunetta et al. (2010)
		(5) Classification and regression trees approach to extract crop types based on MODIS NDVI time-series in Manitoba, Canada	Chen et al. (2016)
		(6) Random Forest classifier to extract crop area in USA based on MODIS time-series	Hao et al. (2015), Zhong et al. (2016)
	Data transform algorithms	(1) Fourier analysis based on MODIS NDVI time-series data to map crop type distribution in northern China	Zhang et al. (2008)
		(2) Wavelet analysis based on MODIS EVI time-series data to map cropland distribution in Mato Grosso, Brazil	Galford et al. (2008)
	Temporal profile fitting method	(1) Temporal best-fitting classifier based on MODIS EVI time-series data to extract crop types in Rondônia, Brazil	Brown et al. (2007)
		(2) Dynamic Time Warping distance-based similarity measure approach based on MODIS NDVI time-series to map cropping system in Vietnam	Guan et al. (2016)
	Phenology Method	(1) Optimizing threshold by comparing key phenology metrics derived from MODIS with that from ground data to extract crop types in central Germany	Xu et al. (2017)
		(2) Quantifying the relationship between crop phenology index time-series and winter wheat area	Pan et al. (2012)
	Hybrid method	(1) Automated Cropland Classification/Mapping Algorithm (ACCA, ACMA) based on clustering classifers and spectro-temporal characteristics from MODIS NDVI time-series	Thenkabail and Wu (2012), Xiong et al. (2017)
		(2) Decision tree algorithms and spectral matching techniques for season rice cropland mapping in Bangladesh and irrigated area mapping in India	Dheeravath et al. (2010), Gumma et al. (2014)
		(3) Object-oriented method and supervised classification to map crop area.	Vintrou et al. (2012)
		(4) Data fusion with Landsat 8 imagery and support vector machine to map crop types in Midwest USA	Zhu et al. (2017)
Subpixel-based approaches	Temporal unmixing technique	(1) Probabilistic temporal unmixing methodology using time-series MODIS red and near infrared data in identifying crop proportion area in northwest Mexico and southern Great Plains, USA	Lobell and Asner (2004)
		(2) Unsupervised signal processing algorithm to temporally decompose MODIS data to automatically map major crop types in Kansas and Nebraska, USA and in Turkey	Ozdogan (2010)
		(3) Spatially constrained phenological mixture analysis (SPMA) to extract crop percent covers using MODIS NDVI time-series data in the Midwest USA	Zhong et al. (2015)
	Regression technique	(1) Regression model with adaptive parameters based on MODIS EVI time-series data to extract winter wheat proportion map in China	Pan et al. (2012)
		(2) Nonlinear regression technique based on MODIS time-series data for mapping fractional corn and soybean distribution at national scale in USA	Chang et al. (2007)
		(4) Linear regression model based on MODIS EVI time-series and Landsat data to produce fractional cropland map in Mato Grosso, Brazil	Zhu et al. (2016)

Note: MODIS, Moderate Resolution Imaging Spectroradiometer; NDVI, normalized difference vegetation index; EVI, enhanced vegetation index; LSWI, land surface water index.

tropical areas. At regional and global scales, many previous studies on cropland mapping used MODIS (Moderate Resolution Imaging Spectroradiometer) data or integration of MODIS and Landsat data to effectively use phenological characteristics from the high temporal resolution (Arvor et al., 2011; Kumar et al., 2008; Lobell and Asner, 2004; Thenkabail and Velpuri, 2006; Wardlow et al., 2007; Xiao et al., 2005). MODIS normalized difference vegetation index (NDVI) and enhanced vegetation index (EVI) time-series data are commonly used for crop classification (Arvor et al., 2011; Gumma et al., 2016; Lobell and Asner, 2004; Ozdogan, 2010; Pan et al., 2012; Thenkabail et al., 2005; Wardlow and Egbert, 2008; Xiao et al., 2005; Zhu et al., 2016, 2017). The approaches can be grouped into two broad categories: pixel-based and subpixel-based methods. Table 1 provides examples for cropland mapping using MODIS time-series data.

Coarse spatial resolution images such as MODIS are often used to map large-scale cropland or single-crop type distribution (Galford et al., 2008; Lobell and Asner, 2004; Teluguntla et al., 2017; Thenkabail and Wu, 2012; Xiao et al., 2005) without taking different cropping patterns and multi-crop types into account. However, the spatial distribution of cropping patterns and crop types at regional and global scales are required for reducing the uncertainty of crop yield estimation and for making better decisions in crop planting to achieve food security. The

development of the spatial distribution of cropping patterns and crop types in Mato Grosso, Brazil, is a challenge due to the following problems: (1) Frequent cloud covers during the crop growing season result in difficulties using crop phenological information. The contaminated pixels may be wrongly recognized as other crop types if the cloud effect is not properly eliminated. (2) Spectral confusion occurs between crop and other artificial vegetation and among crop types. Crops and pastures are often confused due to their similar temporal profiles. Spectral confusion exists among different crop types such as cotton, maize, sugarcane and millet. These crop types have similar agricultural calendars as second crops in a rotation in Mato Grosso (from March to July), thus, most of their temporal profiles may be mixed together, making it hard to extract them. Therefore, this study aimed to develop a new approach to map cropland distribution, identify major cropping patterns (the planting combination of crop types in a given farm area within an agricultural period, e.g., Soy-Maize, and Soy-Cotton), and separate major crop types (the crop category planted within a cropping season, e.g., soy, maize, and cotton) in Mato Grosso, using MODIS NDVI time-series data.

2. Study area

Mato Grosso, the third-largest state in Brazil (over 90,000 km^2), was selected as the study area (Fig. 1a). Mato Grosso contains three major ecobiomes: the Amazon rainforest in the north, Cerrado in the middle, and Pantanal in the south (Dias et al., 2016). Land cover types include forest (primary and secondary forest), plantation (*Eucalyptus*), pasture, high-dense Cerrado with tree-dominant species (CerradoH), low-dense Cerrado with grass-dominant species (CerradoL), crops, water, and impervious surface area (ISA). The agricultural lands are mainly concentrated in the Cerrado biome. The agro-natural landscapes include crop-forest (Fig. 1b) and crop-pasture (Fig. 1c) mosaics. This region has three climate seasons—rainy, dry, and transition season, according to precipitation patterns (Vourlitis et al., 2002). Rainy season ranges from December to March while the dry season occurs approximately from June to September. The remaining months belong to the transition season. Almost all crops are planted in the rainy and transition seasons, except for those growing in the dry season with irrigation. Soy, maize, and cotton are the three main crops in this state, and the agriculture calendar for these crops goes from mid-September to the following July, depending on the soils, regions, and the onsets of rainy and dry seasons (Arvor et al., 2011; Gusso et al., 2014; Zhu et al., 2016). There are two planting periods during an agricultural year. Different crop types are usually combined in separate planting periods. There are six major cropping pattern types: Soy-Maize, Soy-Cotton, Fallow-Cotton, Soy-Fallow, Soy-Pasture, and Single crop (e.g., Cotton-Cotton, Sugarcane-Sugarcane). According to our field survey and statistics from the Brazilian Institute of Geography and Statistics (IBGE), these six cropping patterns account for 93.8% of total agricultural area in Mato Grosso (IBGE, 2015). Therefore, having huge cropland area and different cropping patterns, Mato Grosso is an ideal study area for exploring crop mapping algorithms.

3. Methods

Fig. 2 illustrates the framework of mapping cropland, cropping patterns and crop types using MODIS NDVI time-series data. The major steps include data collection and preprocessing, extraction of phenological features from MODIS time-series data, identification of cropland, cropping patterns, and crop types, and evaluation of the results.

3.1. Data collection and preprocessing

Table 2 summarizes the datasets used in this study, including MODIS NDVI time-series data, Landsat 8 Operational Land Imager (OLI), field survey data, and statistical data of crop types. The 16-day MODIS NDVI composite data (MOD13Q1) with spatial resolution of 250 m was used. During the rainy season, cloud cover is a recurrent problem affecting the real land surface reflectance. The pixels contaminated by clouds and shadows were reconstructed using a simple temporal interpolation method (Chen et al., 2016). Specifically, the contaminated pixels were gap-filled with an interpolation filter by filling with the adjacent non-contaminated values. The major advantage of this method is that the gap-filled value will not break the originality of time series trend composed by clear pixels. The pixel reliability band was used during cloud and shadow detection. After removal of clouds and shadows, all tiles were mosaicked from Sinusoidal to Albers Conical Equal Area projection with the nearest neighbor resampling approach. This projection was selected because it had the minimum bias on the area calculation and the result based on this projection can be used to compare the actual planted area from statistics. All images of each year were layer stacked and subset over Mato Grosso. Finally, the Savitzky-Golay smooth approach was used to eliminate some small fluctuations on the temporal NDVI dataset before running a phenology model (Chen et al., 2004; Savitzky and Golay, 1964).

Two scenes of Landsat OLI imagery in June 2016 were used to validate the crop area extracted from MODIS data. Each Landsat image shows a representative landscape (crop-forest or crop-pasture) to meet the land cover diversity in Mato Grosso. The Landsat 8 L1T product has very good geometric accuracy because it has been systematically terrain-corrected. The two OLI images were first calibrated to top-of-atmosphere reflectance (Mishra et al., 2014), then to land surface reflectance using an improved dark-object subtraction approach (Chander et al., 2009; Lu et al., 2002). A maximum likelihood classifier (MLC) was applied to classify the two Landsat images. The crop map with crop and non-crop categories was generated by grouping forest, pasture, bare soil, water, and ISA into a non-crop category from the MLC classification results. Validation for the crop/non-crop map using 300 points randomly selected by the stratified sampling technique for each image showed that both crop maps have high overall accuracy (higher than 95%) as well as high user's and producer's accuracies (larger than 90%). The accurate Landsat classification results indicated that they could be used as the reference data for validation of the MODIS-derived crop maps.

Land cover samples, collected from field surveys and Google Earth images during the period of September 2015 to August 2016, were used to classify land cover types for MODIS data. Each land cover sample was carefully selected from patches larger than 250 m × 250 m to ensure the purity of samples. A total of 150 samples were collected, and each land cover type has at least 20 samples. Crop type samples were collected from field surveys at Campo Verde municipality in December 2015 and May 2016. A minimum patch size of 25 ha (around 4 pixels) was applied to ensure that the selected patches were sufficiently large to collect a representative spectral-temporal signal. A total of 125 cropping pattern samples were obtained for training with at least five samples for each cropping pattern. The statistical data of crop types include soybean, maize and cotton during the growing season of 2014–2015. It is worth noting that this dataset is a survey, statistics-based at the scale of the municipality.

3.2. Approach to mapping cropland distribution

Many classification algorithms such as MLC, artificial neural network (ANN), support vector machine (SVM), random forest (RF) and decision tree classifier (DTC), are available (see the classification overview by Lu and Weng in 2007). Our research in the Brazilian Amazon indicates that DTC is one of the best classifiers in land cover classification (Li et al., 2012; Lu et al., 2012; Lu et al., 2014). Compared to other machine learning methods such as ANN and SVM that require much time and labor to obtain the optimized parameters, DTC is much easier to interpret and can be built from direct inspection of variables.

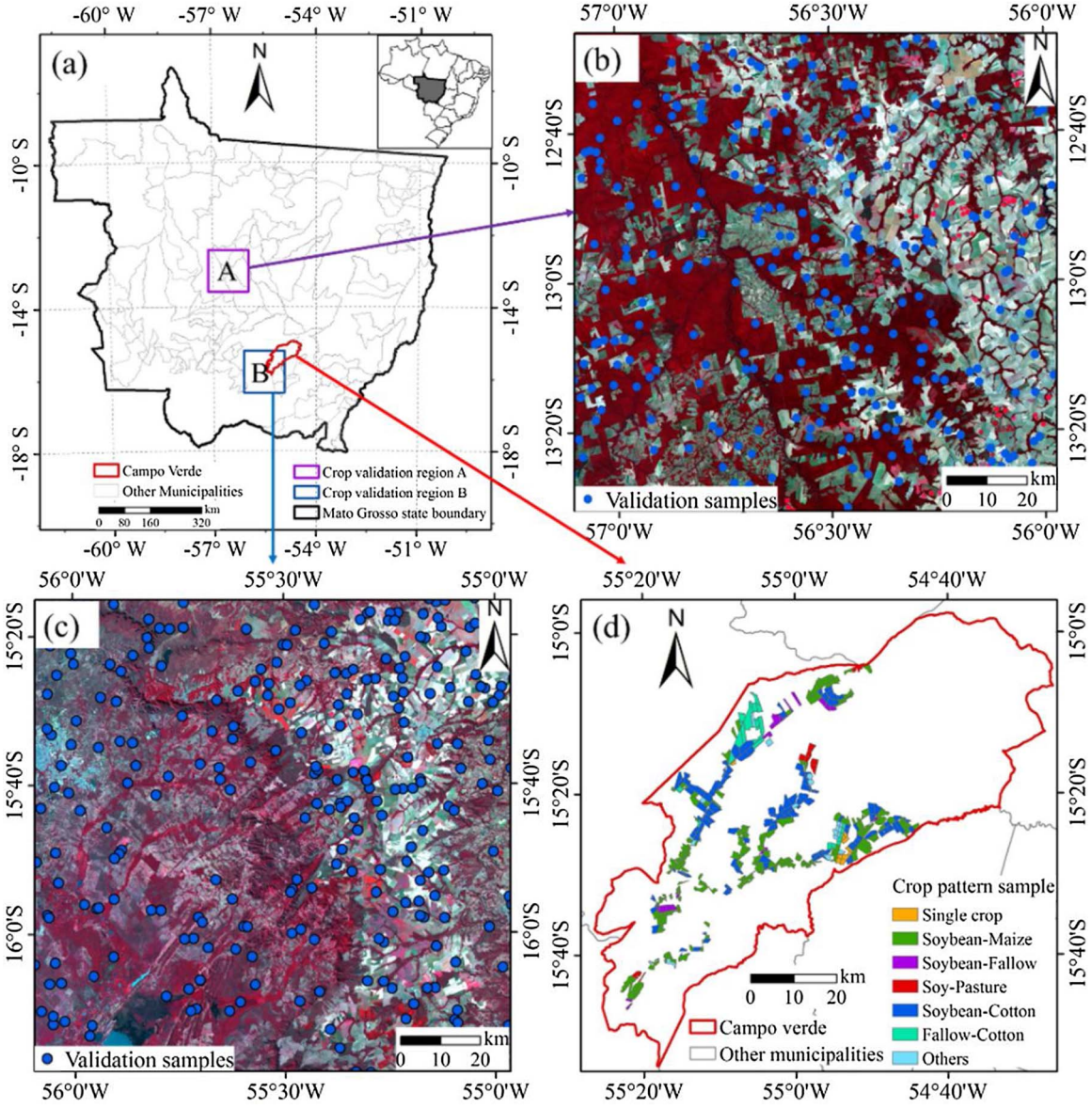

Fig. 1. Study area in Mato Grosso, Brazil (a), crop validation regions A (b) and B (c), and cropping pattern samples in Campo Verde municipality (d).

RF is actually an ensemble of decision trees, thus it is more complex than DTC in terms of parameters predefining, sample training and result voting (Breiman, 2001). Another advantage of using DTC is its explicit working mechanism based on training samples. We coded DTC using MATLAB. One critical step in using DTC is to identify suitable variables and corresponding thresholds for each variable. A comparative analysis of different temporal indices and phenological metrics was conducted to identify variables. Previous research has indicated that phenology features are valuable for land cover classification (Chen et al., 2016; Pan et al., 2012; Xu et al., 2017). Eight land cover types were analyzed based on their temporal patterns of NDVI, and six phenological metrics were calculated from NDVI time-series using the TIMESAT package for each sample (Jönsson and Eklundh, 2004). These metrics include start of season (SOS), end of season (EOS), maximum value, amplitude, base value and length of growing season. SOS is defined as the point on the temporal curve where the distance from the left minimum is 10% of the distance between the left minimum level and the maximum level. Similarly, EOS refers to the point on the temporal curve where the distance from the right minimum is 10% of the distance from the right minimum value and the maximum value. The length of growing season is defined as the time interval between SOS and EOS. Amplitude is defined as the NDVI difference between the maximum NDVI and the base value (Jönsson and Eklundh, 2004).

Fig. 3a illustrates the temporal profile of NDVI mean value (with two times of standard deviation) for each land cover type. Several time points can be used to separate one land cover type from others. For instance, forest and water can be separated by the NDVI values during the dry season in August ($NDVI_{dry}$). However, no single time point can completely extract all crops from other land covers. Fig. 3b, c provides a comparison of six phenology metrics for each land cover type. It indicates that crop is totally mixed with others in terms of SOS, EOS, and length (Fig. 3b), implying these metrics are not suitable for crop extraction. Another three metrics in Fig. 3c indicate that crop is separable from forest, CerradoH, and water but intersects with plantations, pasture, CerradoL, and ISA in terms of base value. Similarly, crop has a much higher maximum value than water and ISA but is mixed with other land covers. In amplitude, crop is isolated from almost all other land covers. Therefore, amplitude and $NDVI_{dry}$ were selected because they had the most potential combination capable of extracting crop. The DTC was then created using these variables (i.e., $NDVI_{dry}$ and amplitude) to extract crop. Average NDVI of all time points from August were used to combine $NDVI_{dry}$. The threshold of $NDVI_{dry}$ was set as 0.25,

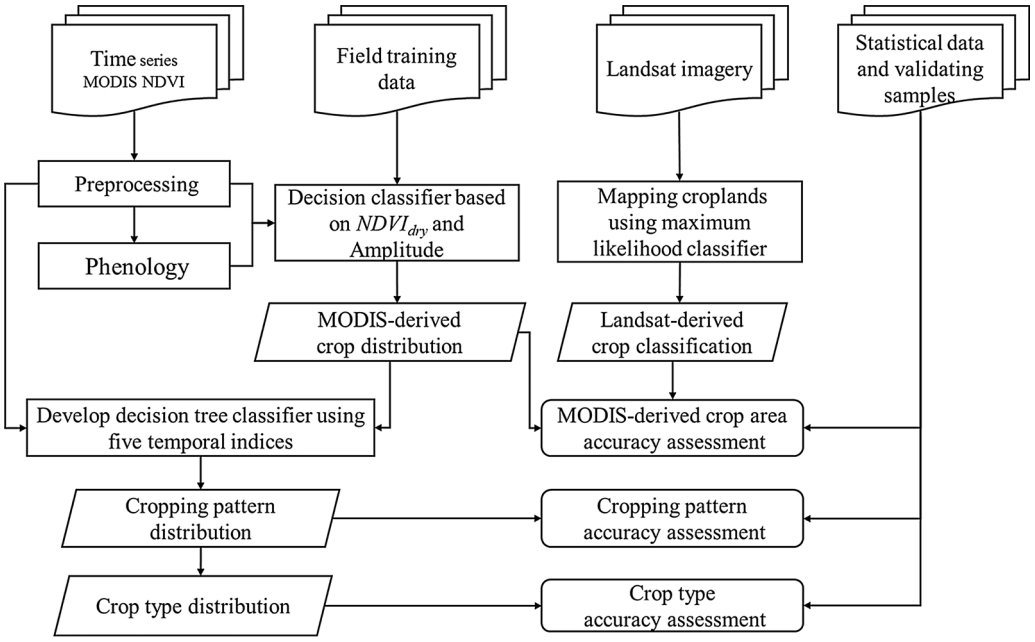

Fig. 2. Framework for extracting croplands, cropping patterns, and crop types from MODIS time-series data. Note: MODIS, Moderate Resolution Imaging Spectroradiometer; NDVI, normalized difference vegetation index.

Table 2
Datasets used in this study.

Data	Spatial resolution	Time period	Source
MOD13Q1 (H12V09, H12V10, H13V09, H13V10)	250 m	MODIS time-series data between 9/2014 and 8/2016	https://ladsweb.nascom.nasa.gov/index.html
Landsat Operational Imager (Path/Row: 227/69 & 226/71)	30 m	Two images on 6/13/2016 and 5/5/2016	https://earthexplorer.usgs.gov/
Land cover and cropping pattern samples	–	2015–2016	Field survey in May 2016, Google Earth images
Area statistics of crop types	Yearly, 142 municipalities	2014–2015	Brazilian Institute of Geography and Statistics (IBGE)

Note: MODIS, Moderate Resolution Imaging Spectroradiometer.

which was determined as the middle value between the upper bound of water and bottom bound of crop. Similarly, the threshold of amplitude was set as 0.4, which was determined as the middle value between the bottom bound of crop and upper bound of CerradoH. Finally, the crop areas in 2015 and 2016 were produced by implementing the DTC.

3.3. Approach to mapping cropping pattern and crop type distribution

Each cropping pattern has its own characteristics in the stages of planting, growing, and harvesting. This provides the possibility of extracting cropping pattern types using remote sensing time-series imagery. In reality, temporal profile analysis of crop phenology is fundamental for crop type mapping. Fig. 4a illustrates the NDVI temporal profiles based on six cropping patterns in Mato Grosso. Although selected cropping patterns have similar NDVI values in particular periods, some differences can still be used to distinguish them. For example, a single cropping system has only one peak stage while the double cropping system has two peak stages, implying that the number of peaks can be used to extract a single cropping pattern from a double cropping pattern. The peak value of Fallow-Cotton pattern during its fallow season is much smaller than that of the other four double-cropping patterns during the same period, indicating the peak value in the first season is a potential variable to extract Fallow-Cotton pattern. Since the NDVI value of Soy-Pasture in the late dry season is much higher than that of Soy-Maize, Soy-Cotton, and Soy-Fallow in the same period, the NDVI value in this period can be used to separate Soy-Pasture from other patterns. The harvest of soy in Soy-Cotton patterns occurs earlier than in Soy-Maize, Soy-Fallow and Soy-Pasture, resulting in smaller NDVI values of Soy-Cotton than others during the same period, while the harvest of maize in Soy-Maize occurs earlier than the harvest of cotton in Soy-Cotton and the senescence of fallow vegetation in Soy-Fallow in the second crop season, leading to smaller NDVI values of Soy-Maize in the same period. Thus, NDVI values at the ends of the first and second crop seasons can be used as potential variables. In summary, five temporal indices can be used to identify all cropping patterns over the study area: number of peaks (NOP), peak values in the first season (PVFS), values in the late dry season (VLDS), values in the harvest period of the first season (VHPFS), and values in the harvest period of the second season (VHPSS).

Fig. 5 illustrates the strategy of using DTC based on five temporal indices to classify cropping patterns. According to the statistics shown in Fig. 4, the following thresholds were determined:

(1) If NOP of a cropland pixel equals one, this pixel is assigned as a single cropping pattern;
(2) If PVFS of a cropland pixel is less than 0.52, this pixel is assigned as Fallow-Cotton;
(3) VLDS was used to identify Soy-Pasture pattern. Two temporal points on August 28 and September 14 were selected to combine VLDS because these NDVI values have the largest differences from the other four types. If VLDS is greater than 0.44 (see Fig. 4c), this pixel is assigned as Soy-Pasture;
(4) VHPSS and VHPFS were used to identify Soy-Maize and Soy-Cotton. VHPSS included values on June 9 and 25 and July 11 and VHPFS

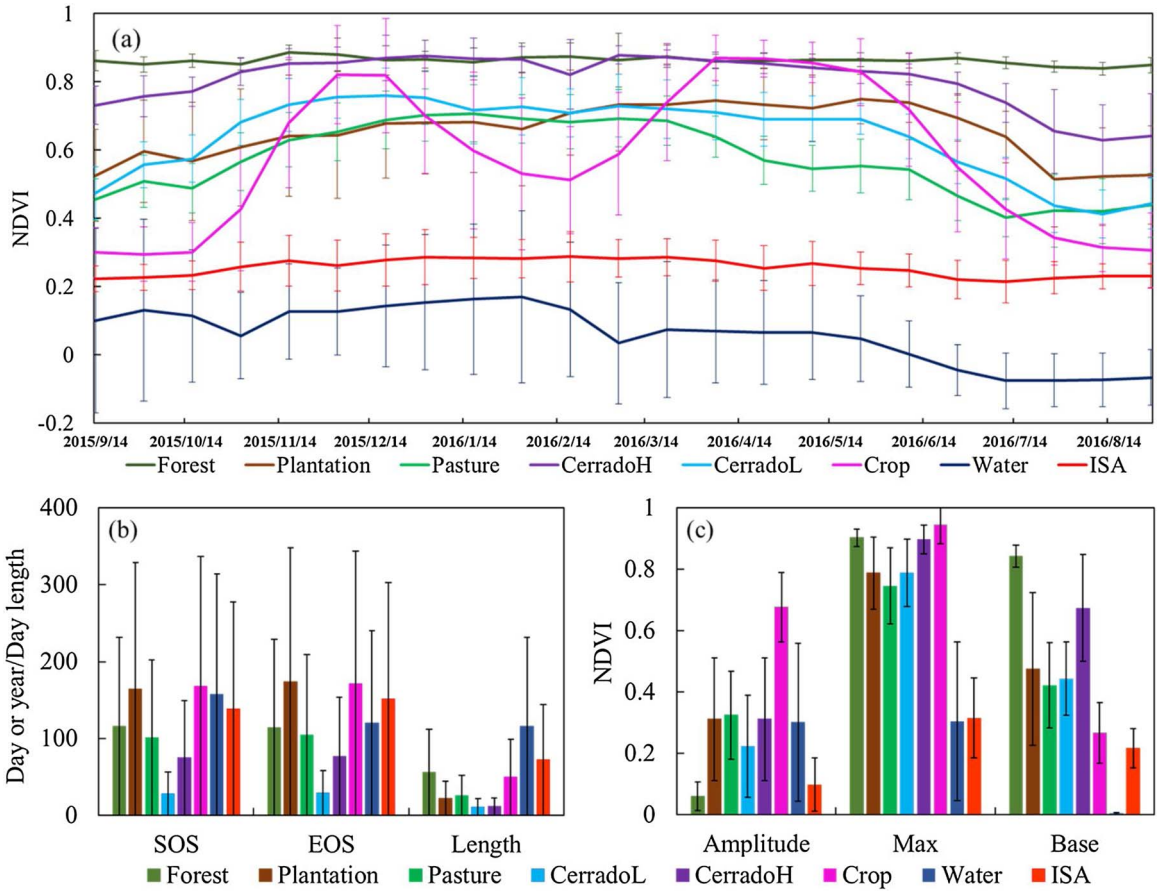

Fig. 3. Temporal profiles (a) and phenology features (b and c) of land cover types in Mato Grosso, Brazil. Note: NDVI, normalized difference vegetation index; SOS, start of season; EOS, end of season.

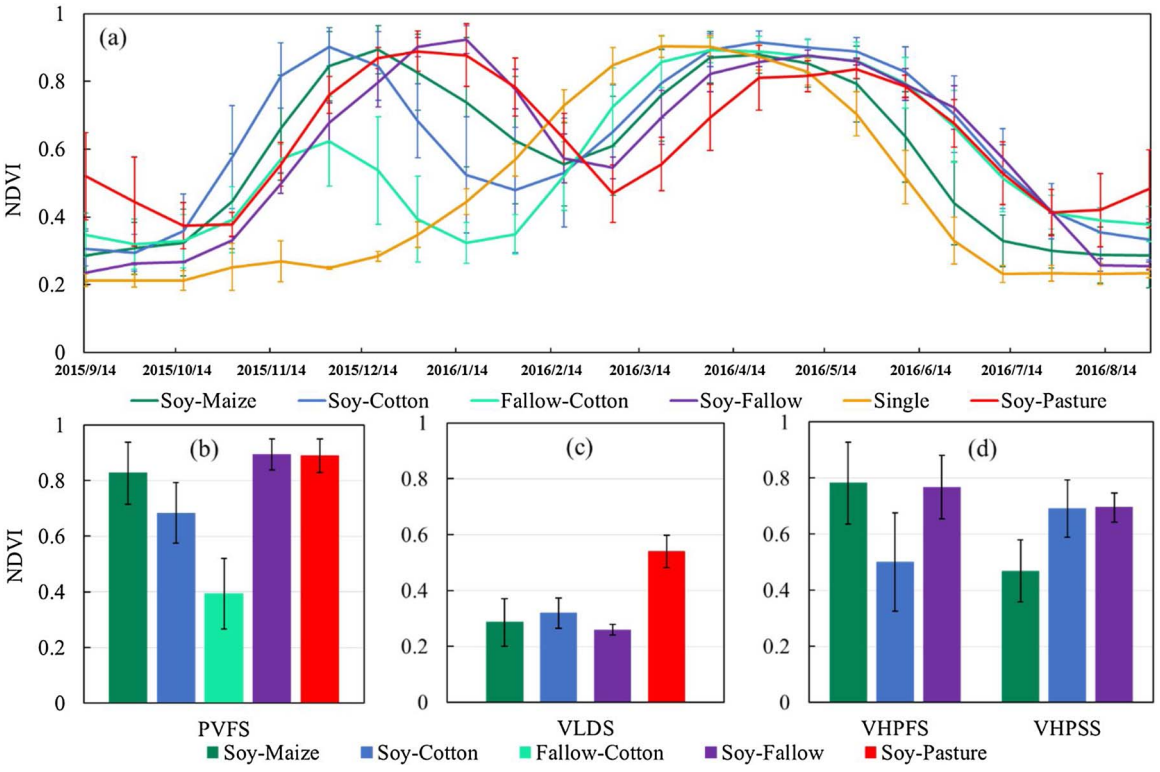

Fig. 4. Temporal profiles (a) and phenological features (b, c, and d) of cropping patterns in Mato Grosso, Brazil. Note: PVFS, peak values in the first season; VLDS, values in the late dry season; VHPFS, values in the harvest period of first season; VHPSS, values in the harvest period of second season.

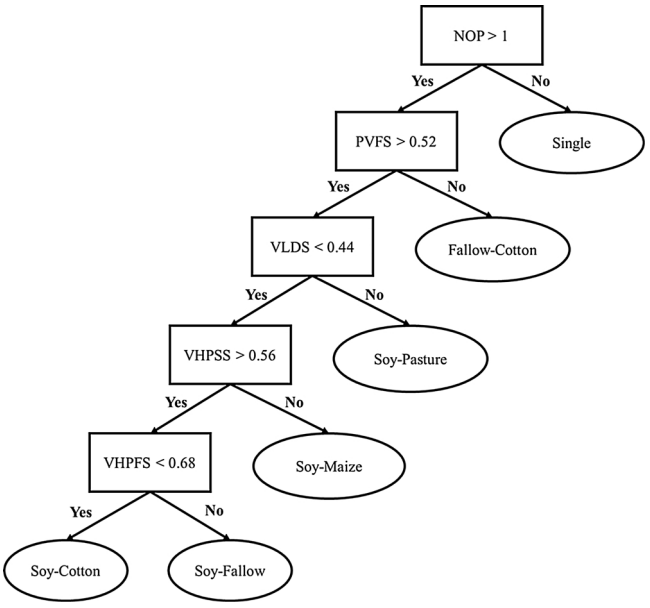

Fig. 5. Decision tree rules of cropping pattern classification in Mato Grosso, Brazil. Note: NOP, number of peaks; PVFS, peak values in the first season; VLDS, values in the late dry season; VHPFS, values in the harvest period of the first season; VHPSS, values in the harvest period of the second season.

included values on January 17 and February 2 according to the agricultural calendar in Mato Grosso. Thresholds of VHPSS and VHPFS were set as 0.56 and 0.68, respectively, according to the statistics of Fig. 4d. Here VHPSS is first applied because it has more identical intervals for Soy-Maize than VHPFS for Soy-Cotton. The threshold of VHPFS is set higher than the upper bound of Soy-Cotton to include more pixels for Soy-Cotton because it is one of the primary cropping pattern types in Mato Grosso.

It is worth noting that all thresholds were optimized by changing their values within a certain range, which was determined by the NDVI ranges of cropping patterns. The cropping pattern maps of the agricultural years of 2015 and 2016 were generated after implementing the proposed DTC. After the cropping pattern distribution was obtained, the crop types were transformed using the following equations:

$$Soy = Soy\text{-}Maize + Soy\text{-}Cotton + Soy\text{-}Fallow + Soy\text{-}Pasture + Single \quad (1)$$

$$Maize = Soy\text{-}Maize \quad (2)$$

$$Cotton = Soy\text{-}Cotton + Fallow\text{-}Cotton \quad (3)$$

Although single cotton and single maize have co-existed in Mato Grosso in recent years, the single cropping system was characterized by soy in this study. This is because (1) according to the 2015 statistical data from IBGE, the planted areas of total cotton and first crop maize accounted for only 5.45% and 0.62% of total crop area, respectively, implying that the planted areas of single cotton and first crop maize are much smaller than the areas of single soy and first crop soy; (2) most single maize patches are too small to be classified using MODIS data. Similarly, other double cropping systems such as Maize-Cotton were not considered in this study for the same reason. These assumptions are also found in Arvor et al. (2011) and Brown et al. (2013). Details about the uncertainties and bias resulting from these assumptions are discussed in Section 5.

3.4. Evaluation of cropland, cropping pattern and crop types

The error matrix is commonly used to evaluate classification results (Congalton and Green, 2008) and was used in this research. However, the evaluation of classification results from coarse spatial resolution data is difficult due to land cover heterogeneity. Two approaches based on Landsat image classification and statistical data were used in this research. The MODIS-derived cropland map for 2016 was evaluated using the cropland data from Landsat in the same year. The MODIS-derived cropping pattern map and crop type map for 2016 were evaluated using the field survey data. The MODIS-derived cropland area and crop type area for 2015 were evaluated using statistical data from the same year.

Determination of the number of test samples and the method to allocate these samples were critical for conducting the correct accuracy assessment (Lu and Weng, 2007). Generally, the number of test samples is based on the expected percent accuracy and allowable error (Congalton and Green, 2008) or based on the rule of thumb that one needs a minimum of 50 test samples for each class. In this research, the crop/non-crop data from Landsat with 30-m cell size were aggregated to 250-m cell size, the same as MODIS data, using the majority approach. A total of 300 test samples were selected from the aggregated crop distribution images at two sites using the stratified random sampling approach. These test samples were used to evaluate the MODIS-derived cropland maps. A total of 262 test samples for cropping patterns were selected from the field survey and these test samples were different from the training samples. For crop types, the test samples were derived from the cropping-pattern test samples by applying rules shown in Eqs. (1)–(3). The error matrix was then developed for the cropland, cropping pattern and crop type classification result, respectively. Finally, overall accuracies, user's accuracies, and producer's accuracies for cropland, cropping pattern and crop type were calculated from the error matrix respectively (Foody, 2009).

Another approach to evaluate the MODIS-derived results is based on statistical data at the municipality level. The reference data for cropland and crop type areas were calculated from IBGE data for each municipality. The MODIS-derived cropland and crop type areas for each municipality in Mato Grosso were calculated using a zoning statistical technique. The normalized difference area index (NDAI), adjusted coefficient of determination (R^2), and relative root mean square error (RRMSE) (Wang et al., 2012) were used to evaluate the MODIS-derived results. The equations are expressed as follows:

$$NDAI_i = (E_i - S_i)/(E_i + S_i) \quad (4)$$

$$R'^2 = 1 - \sum_{i=1}^{n} (S_i - E_i)^2 / \sum_{i=1}^{n} (S_i - \overline{S})^2 \quad (5)$$

$$R^2 = 1 - (1 - R'^2)\frac{n-1}{n-p-1} \quad (6)$$

$$RRMSE = \sqrt{(\Sigma_{i=1}^{n} (E_i - S_I)^2)/n} \times \frac{100}{5} \quad (7)$$

where E_i and S_i are estimated area and statistical area in municipality i, respectively; $\overline{E}$ and $\overline{S}$ are the averages of the estimated area and statistical area of all municipalities, respectively; p and n represents the total number of independent variables and samples (municipalities), respectively. R'^2 represents the coefficient of determination. Compared to R'^2, R^2 is more general because it eliminates the influence derived from samples and independent variables. NDAI reflects the deviation extent (-1 to 1) of the estimated area to the reference data; that is, a negative value implies an underestimation and a positive value an overestimation, and the closer the value is to zero means the higher accuracy of the estimation.

4. Results

4.1. Analysis of cropland mapping results

The developed cropland distribution from MODIS data (Fig. 6) indicates that the croplands are mostly distributed in central and southeastern Mato Grosso, accounting for 14.68% of the total land in this

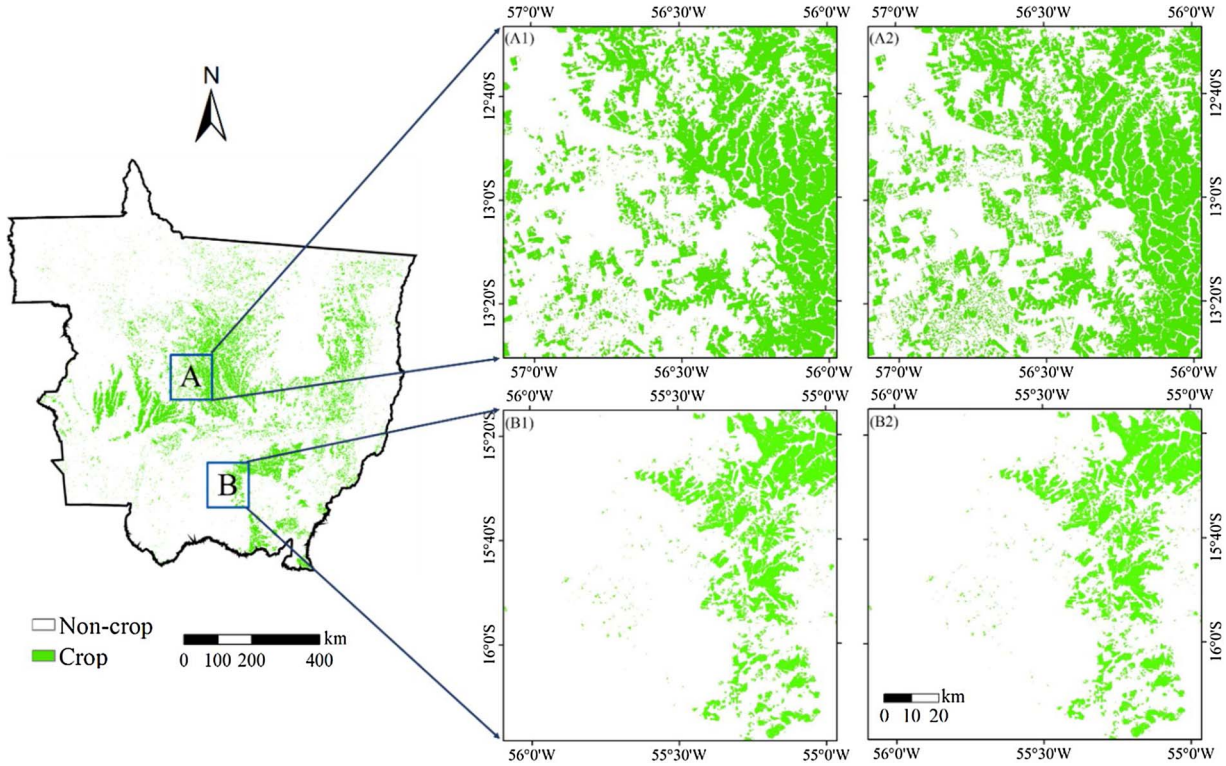

Fig. 6. Comparison of cropland distributions between the MODIS-derived map (A1 and B1) and Landsat-derived map (A2 and B2) in two test regions (A and B) in Mato Grosso, Brazil.

state. The cropland distributions from MODIS data (A1 and B1) match well with the results from Landsat data (A2 and B2) for two test regions. The locations with larger cropland patch sizes (right side in A1 and A2, and top right in B1 and B2) have higher consistency than the locations with fragmented patches (left sides in A and B). Thus, landscape configuration has an important impact on cropland mapping accuracy.

The accuracy assessment result (Table 3) indicates that croplands in Mato Grosso can be effectively mapped from MODIS images with an overall accuracy of over 90%. However, misclassification existed in both test regions. For example, other classes in test region A were misclassified as croplands, and the cropland class was misclassified as other classes in test region B. This is because the fragmented fields may be classified as non-cropland (in region A) or cropland (in region B), depending on the composition of land covers, due to the similar temporal signals between crop and pasture. Note that the user's accuracy in region A (95.4%) is higher than in region B (78.0%). This further confirmed the impacts of the landscape structure on cropland extraction. Obviously, it is more difficult to extract cropland from crop-pasture landscapes in region B than crop-forest landscapes in region A, as pasture has more phenological and spectral signals similar to crops than forest. Overall, the proposed approach for cropland mapping based on MODIS NDVI time-series data is able to successfully extract croplands over large areas.

The adjusted coefficient of determination (R^2) between MODIS-derived cropland and statistical data in 2015 at the municipality scale was 0.94 (Fig. 7a), implying the promise of this approach in developing croplands from MODIS data. Note that the regression line of cropland almost overlaps at the 1:1 diagonal, further confirming the high agreement between the cropland area estimation and statistical data. Fig. 7b shows the inconsistency sources that cropland estimation errors decreased as the planted area at municipality scale increased. That is, the smaller cropland areas in the municipalities resulted in higher estimation errors. Around 20 municipalities with very small cropland areas have NDAI values of 1, which is reasonable due to the mixed pixels dominated by smaller cropland areas in MODIS data. Consequently, the higher estimation errors result from misclassification of these mixed pixels when pixel-based approaches are used. Fig. 7b also indicates that overestimation of cropland areas is dominant in most municipalities as most NDAI values are larger than 0. Municipalities with small cropland areas are more prone to be overestimated. In order to better visualize the overestimation in those municipalities, Fig. 8 provides examples of municipalities where the crop areas are small and overestimated.

Table 3
Confusion matrix and accuracy statistics for croplands derived from the 2016 MODIS imagery in Mato Grosso, Brazil.

		Reference data from Landsat classification results				
		Cropland	Others	Total	Producer's accuracy	User's accuracy
Region A	Cropland	103	5	108	85.12	95.37
	Others	18	174	192	97.21	90.63
	Total	121	179	**Overall accuracy**: 92.33%		
Region B	Cropland	78	22	100	90.7	78
	Others	8	192	200	89.72	96
	Total	86	214	**Overall accuracy**: 90%		

4.2. Analysis of cropping pattern mapping results

An overall accuracy of 73% for cropping patterns (Table 4) was obtained. All cropping patterns, except Soy-Fallow, have user's accuracies of 78% or higher and producer's accuracies of 66% or higher. Single-crop has the highest accuracy with the smallest commission and omission errors. This is reasonable because the temporal profile of the Single-crop (Fig. 4) is considerably different from that of other cropping patterns. Almost half of Soy-Fallow samples were wrongly classified as Soy-Maize and Soy-Cotton, resulting in a very low user's accuracy (30%). This is mainly caused by the difficulty in separating the highly mixed spectral characteristics among these three cropping patterns as indicated in Fig. 4. This difficulty also results in some Soy-Maize

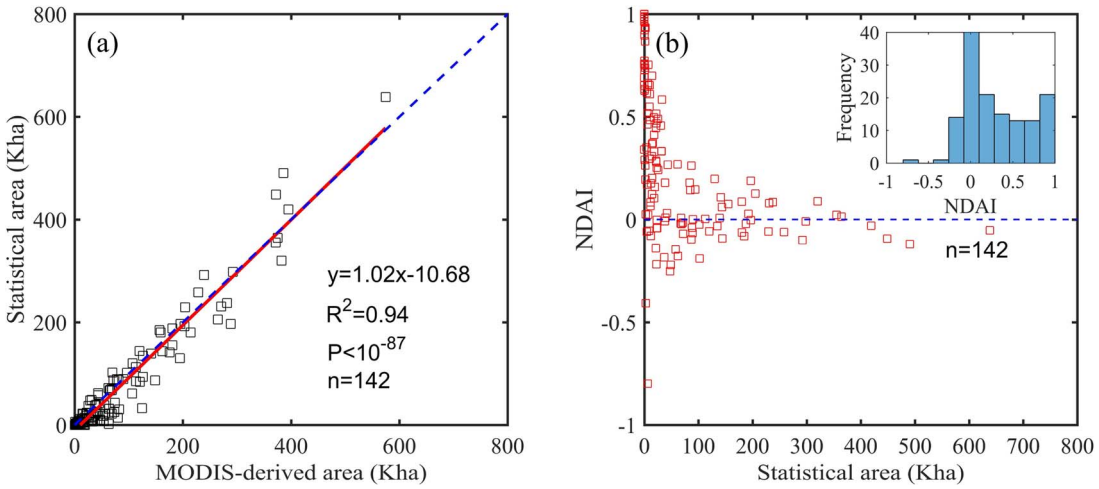

Fig. 7. Comparison of MODIS-derived cropland areas and statistical data (a) and analysis of normalized difference area index (NDAI) of croplands with statistical data (b) at the municipality scale in Mato Grosso, Brazil.

samples being wrongly classified as Soy-Cotton and Soy-Fallow.

The spatial distribution of cropping patterns in Mato Grosso in 2015 (Fig. 9) indicates that Soy-Maize was mainly concentrated in the Cerrado biome, in the center of the state, and Soy-Fallow was largely distributed in the west and south parts. Soy-Cotton and Fallow-Cotton were mainly clustered in the west and southeast and Single crop and Soy-Pasture were scattered throughout the state. Further analysis of the cropping pattern areas (Table 5) indicates that Soy-Maize had the largest area in 2015, accounting for 39% of the total cropland area, followed by Soy-Fallow with 31%. Single crop and Soy-Pasture had similar planted area, occupying around 12% of total crop area. Soy-Cotton and Fallow-Cotton had the smallest areas with 2%–3% of total crop area each.

4.3. Analysis of crop type mapping results

An overall accuracy of 86% of crop types (Table 6) indicates that the proposed method can successfully extract Soy, Maize and Cotton in Mato Grosso. Soy has the best accuracy with user's accuracy of 94% and producer's accuracy of 96%, much higher accuracy than that of Soy-related cropping patterns as indicated in Table 4. This is because these four Soy-related cropping patterns – Soy-Maize, Soy-Cotton, Soy-Fallow and Soy-Pasture are highly mixed in cropping pattern mapping (Table 4), but when they are merged into one (soy) in crop type mapping, the accuracy of soy is improved. The similar situation is for maize and cotton.

The relationship between MODIS-derived crop type areas and statistical data in 2015 (Table 7) shows high R^2 values for soy, maize, and cotton, implying that the MODIS-derived areas for different crop types have strong agreements with corresponding statistical data. The estimated total cropland area reached 11,122 kha (kilo hectare), approximately 281 kha higher than the statistical cropland area. The high R^2 values (0.94) and low RRMSE value (35%) further prove that the proposed approach can effectively extract cropland area at large-scale using MODIS data. The similar conclusion is for soy with RRMSE of 31.7%.

The relationship between MODIS-derived crop type area and corresponding statistical data (Fig. 10a1,b1,c1) shows a conclusion similar to results in Table 7; that is, soy has the best estimation results. The scatterplot between NDAI and statistical data for each crop type (Fig. 10a2,b2,c2) indicates that soy and maize had many NDAI values of nearly 0, implying that they have high extraction accuracies. In contrast, cotton has an NDAI value of 1 in many municipalities (Fig. 10c2), indicating poor estimation. Fig. 10 also shows how the smaller areas estimate deviate from their statistical values. Fig. 10a2 indicates that soy is prone to be overestimated when soy areas in the municipalities are less than 50 Kha. Fig. 10b2 indicates maize has a similar number of overestimated and underestimated municipalities. Fig. 10c2 indicates cotton is mainly underestimated for the municipalities with cotton areas larger than 10 Kha, and overestimated when cotton areas are smaller than 10 kha.

The spatial distribution of crop types in Mato Grosso in 2015 (Fig. 11a) indicates that the soy distribution is very similar to the cropland distribution (Fig. 6). Maize appears in the Soy-Maize pattern, and cotton occurs at both Soy-Cotton and Fallow-Cotton patterns (Fig. 11b vs. Fig. 9). Analysis of each crop type area (Table 8) indicates that soy has the largest planted area in Mato Grosso, accounting for 98% (69%) of the total cropland area (total crop type area), and cotton has the least, accounting for only 5% of total cropland area. Note that the percentages of crop type areas are more than 100% because of the double cropping systems.

5. Discussion

This research proposed a new approach to map cropland, cropping pattern and crop type distributions using MODIS time-series data. One key to identify cropping patterns is to examine the differences of phenological variables among crop types. The DTC for extracting croplands and cropping patterns is simple and easy to implement and the results are promising. Besides major cropping patterns like Soy-Maize and Soy-Cotton, this proposed method is able to identify Crop-Fallow and Crop-Pasture, something that previous research has not explored (Arvor et al., 2011; Brown et al., 2013).

Different factors, such as cloud- and shadow-contaminated pixels, temporal interpolation, smoothing, spatial sampling, assumptions for the cropping and mixed pixels, may affect the cropping pattern and crop type mapping results. Although the 16-day MODIS NDVI composite and the temporal interpolation removal algorithm have been used to remove the clouds and shadows, some omitted contaminated time points still exist in the rainy season. The pixels with undetected cloud temporal points could be incorrectly classified because of the mixed pixels in the temporal indices. The temporal interpolation of cloud pixels also brings uncertainty if the interpolation is over-adjusted. The Savitzky-Golay smoothing filter can reduce some disturbances from clouds but could also filter some important points. The uncertainties derived from our temporal interpolation, smoothing, and spatial sampling should be further analyzed. Although the nearest neighbor resampling method does not change the originality of NDVI values, it also cannot reflect the actual values for the sampled pixels. The inconsistent geographic locations between MODIS and Landsat (around 50 m at best

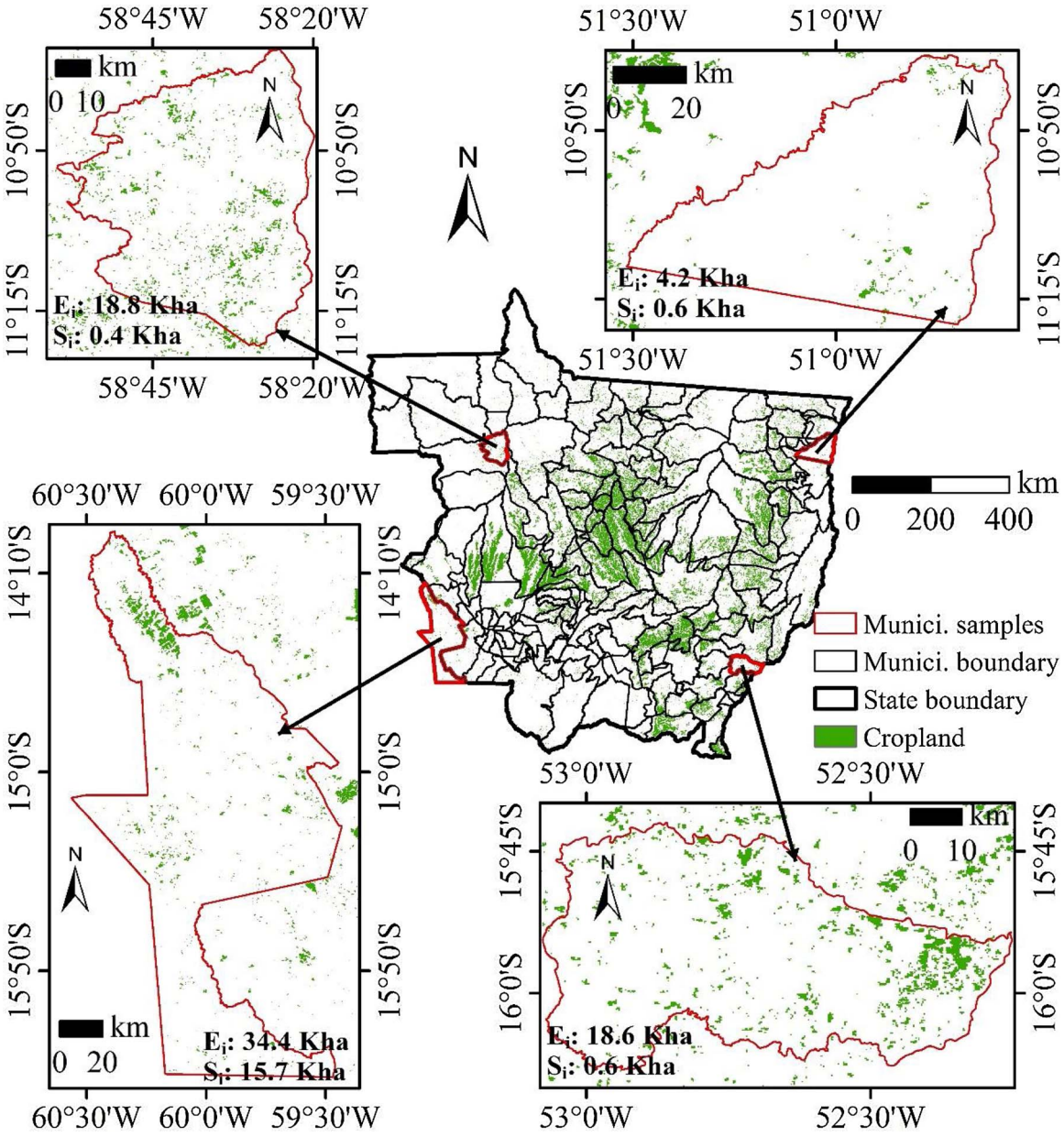

Fig. 8. Visual examples of municipality whose cropland area is overestimated comparing to statistical data.
(*Note*: Munici. represents municipality.).

position) can also cause errors in the overall accuracy (Chen et al., 2016).

The thresholds used for extraction of the croplands and cropping patterns came from typical sample plots, but the determination of these thresholds is subjective; that is, the estimated areas may change when thresholds are different. This research indicates that the municipalities with small cropland areas have high estimation errors—small cropland patch sizes (mixed pixels in MODIS data) resulted in high uncertainty in

Table 4
Confusion matrix and accuracy statistics for cropping patterns derived from the 2016 MODIS imagery in Mato Grosso, Brazil.

	Reference class						Total	UA	PA	OA
	Soy-Maize	Soy-Cotton	Soy-Fallow	Soy-Pasture	Fallow-Cotton	Single				
Soy-Maize	62	6	7	1	2	1	79	78%	79%	73%
Soy-Cotton	2	57	1	0	4	1	65	88%	70%	
Soy-Fallow	11	12	14	5	3	2	47	30%	61%	
Soy-Pasture	2	1	1	17	0	0	21	81%	74%	
Fallow-Cotton	1	4	0	0	21	1	27	78%	66%	
Single	0	1	0	0	2	20	23	87%	80%	
Total	78	81	23	23	32	25	262			

Note: UA, PA, and OA represent user's accuracy, producer's accuracy, and overall accuracy.

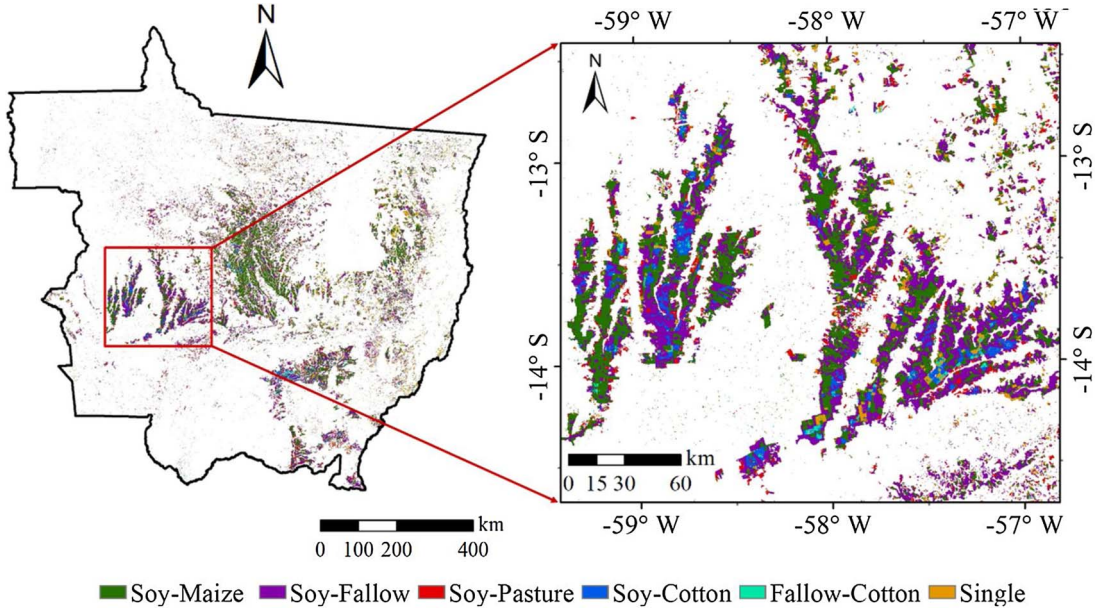

Fig. 9. Spatial distribution of cropping patterns in Mato Grosso, Brazil, in 2015.

Table 5
Areal statistics of MODIS-derived cropping patterns in Mato Grosso, Brazil, in 2015.

	Soy-Maize	Soy-Fallow	Soy-Pasture	Soy-Cotton	Fallow-Cotton	Single crop
Area (kilo hectare)	4,353.7	3,476.4	1,366.0	327.5	229.0	1,370.0
% in cropland area	39.15	31.26	12.28	2.94	2.06	12.32

Table 6
Accuracy assessment result for crop types derived from the 2016 MODIS imagery in Mato Grosso, Brazil.

	Reference class				Total	User's accuracy	Producer's accuracy	Overall accuracy
	Soy	Maize	Cotton	Others				
Soy	224	0	3	11	238	94%	96%	86%
Maize	1	62	8	8	79	78%	79%	
Cotton	2	3	86	1	92	93%	76%	
Others	6	13	16	58	93	62%	74%	
Total	233	78	113	78	502			

Table 7
Areal comparison between MODIS-derived and statistical croplands and crop types in Mato Grosso, Brazil, in 2015.

Crop type	MODIS-derived estimation (Kha)	Statistical area (Kha)	R^2	RRMSE
Soy	10,893.35	8966.68	0.94	31.71
Maize	4353.49	3570.61	0.88	59.25
Cotton	556.53	590.51	0.88	40.68
Total cropland area	11,122.39	10,840.54	0.94	35.01

Note: Kha, kilo hectare; adjusted coefficient of determination (R^2).

area estimation of croplands and crop types. This situation is consistent with previous research (Chen et al., 2016) showing that pixel homogeneity is an important factor in crop area mapping. The impact of mixed pixels can be ignored in the municipalities having large cropland area, but cannot be ignored in those municipalities with small cropland areas. Due to the difficulty in identifying small cropland patches and small areal proportion, single maize, single cotton, and Maize-Cotton cannot be extracted in this study. This may cause overestimation for soy area and other double cropping systems and bias of crop type assessment based on statistical data. More research should be focused on the improvement of estimation accuracy for the regions with relatively small patch sizes.

Much research has explored the approaches to reduce the impacts of mixed pixels on land cover mapping accuracy (Lobell and Asner, 2004; Ozdogan, 2010; Zhu et al., 2016, 2017). Spectral mixture analysis has proven to be an effective tool to decompose mixed pixels into fractional objects (Kumar et al., 2008; Lobell and Asner, 2004; Ozdogan, 2010) and has been extensively used in medium spatial resolution images such as Landsat imagery (Chen et al., 2015; Lu et al., 2003). For coarse spatial resolution images such as MODIS data, the difficulty is in selecting suitable endmembers. An alternative is to use data fusion techniques to integrate Landsat and MODIS data to improve the spatial resolution of datasets. However, the huge amount of data needed will be a challenge in a large area. Another solution could be the development of approaches to map fractional cropland distribution by using estimation models based on the relationships between MODIS vegetation index and Landsat-derived cropland data (Zhu et al., 2016, 2017). The regression-based approach to estimate fractional cropland distribution is a solution to improve area estimation (Zhu et al., 2016), but future research should be on the development of a suitable approach to estimate fractional areas for different crop types or crop patterns,

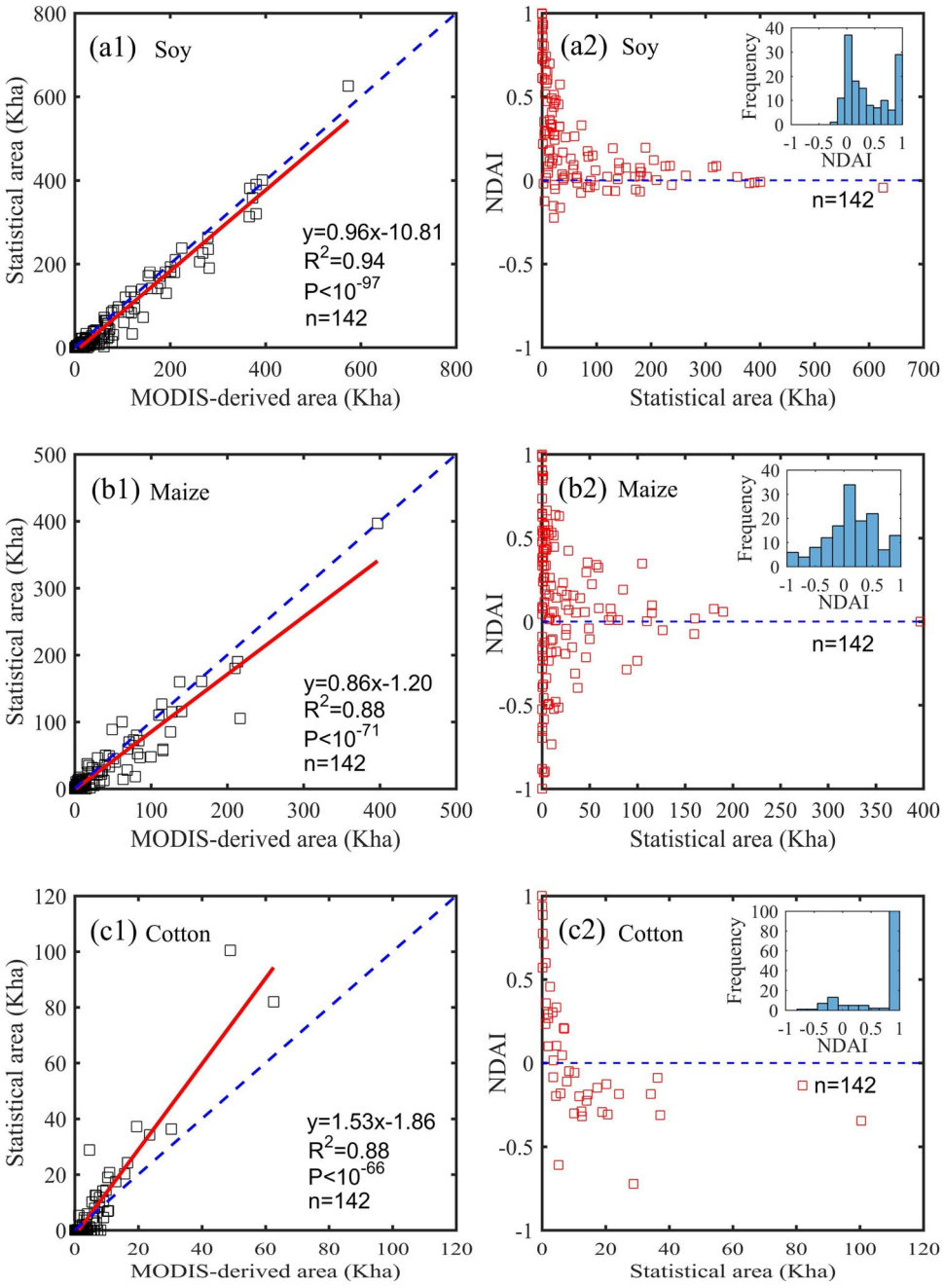

Fig. 10. Areal comparison of crop types from the MODIS and Statistic data (a1: soy; b1: maize; c1: cotton) and analysis of normalized difference area index (NDAI) of crop types (a2: soy; b2: maize; c2: cotton) at the municipality scale.

especially for places with relatively small patch sizes of crop distribution.

Collection of cropping pattern ground-truth data over the whole state is a challenge. During field work, our collected cropping pattern data were mainly located within Campo Verde municipality, but no samples for other regions were available. Given the high crop heterogeneities in municipalities with small crop areas, their accuracy of cropping patterns and crop types could be lower than the accuracy in Campo Verde. The developed approach based on samples and MODIS datasets for 2016 was transferred to the 2015 data for cropping pattern mapping in Mato Grosso, and the results have shown a good agreement when the evaluation was conducted at municipality scale based on the statistical data. However, caution should be taken when the developed approach is directly transferred to other study areas because of the different landscapes and land cover compositions. Adjustment of the thresholds used in the DTC may be needed, depending on the cropping pattern samples in a specific study.

6. Conclusions

A new approach was developed to map cropland, cropping pattern and crop type distributions using MODIS NDVI time-series data in Mato Grosso, Brazil. The major steps included (1) reconstructing MODIS NDVI time-series data by removal of contaminated pixels using the temporal interpolation algorithm; (2) identifying the best periods and developing temporal indices and phenological parameters to extract croplands; and (3) developing crop temporal indices to extract cropping patterns and crop types using NDVI time-series data. Decision tree classifier was applied to extract cropping patterns. The results show that the proposed approach can effectively extract croplands, cropping

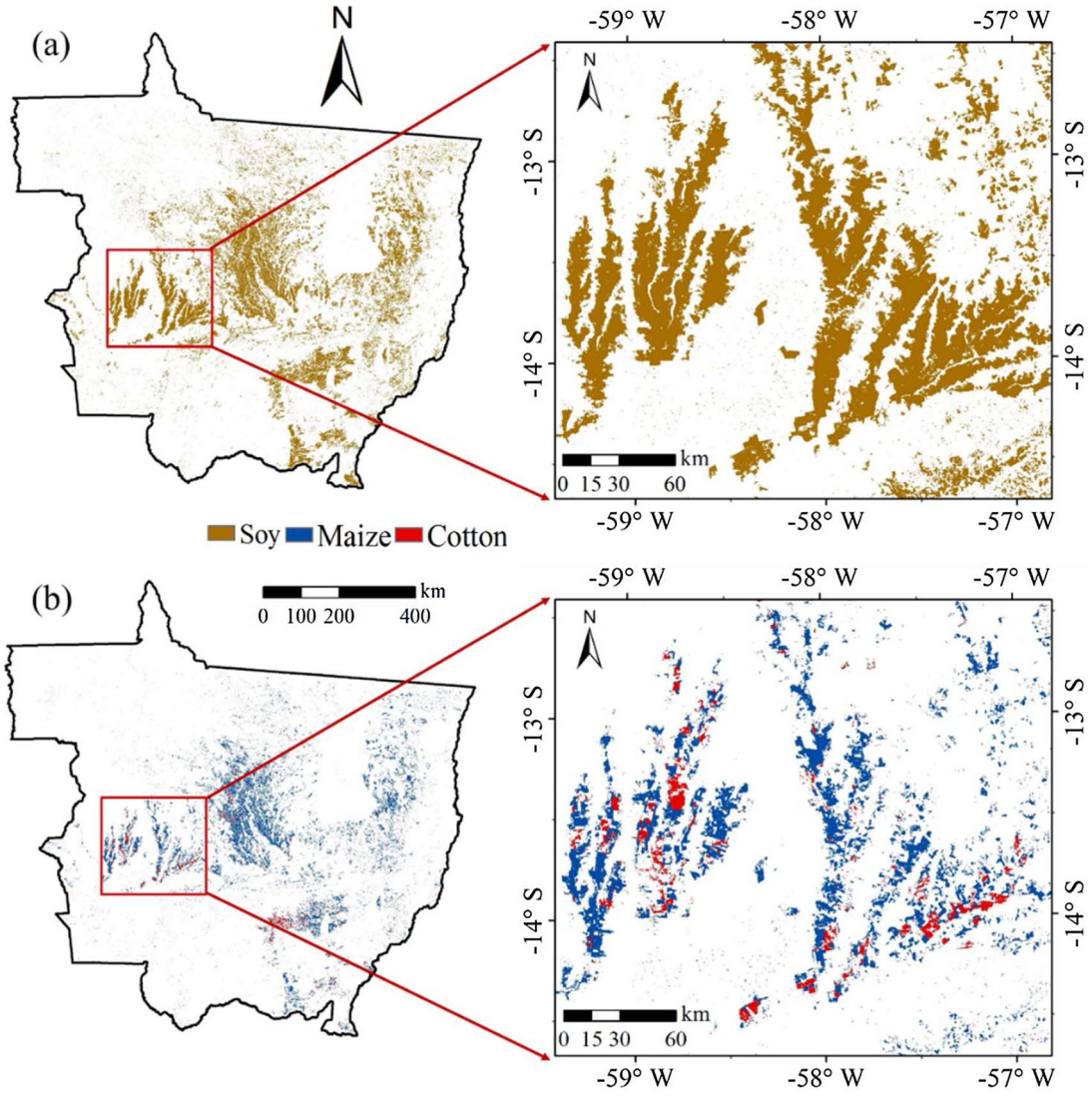

Fig. 11. Spatial distribution of crop types in Mato Grosso, Brazil, in 2015: soy (a) and maize/cotton (b), noting the overlapped areas due to a double cropping system.

Table 8
Areal statistical results of MODIS-derived crop types in Mato Grosso, Brazil, in 2015.

	Soy	Maize	Cotton
Area (kilo hectare)	10,893.35	4353.49	556.53
% in total cropland area	97.94	39.14	5.00
% in total area of crop types	68.93	27.55	3.52

patterns and crop types. Overall accuracies of MODIS-derived croplands, cropping patterns and crop types are around 90%, 73% and 86%, respectively. In order to test the reliability of the developed approach, this method was transferred to 2015 for cropping pattern mapping in Mato Grosso. The R^2 values between MODIS-derived data and statistical data for soy, maize, cotton, and cropland were 0.94, 0.88, 0.88 and 0.94, respectively. This research will be valuable for rapidly updating croplands, cropping patterns, and crop types over large areas, especially in regions having large cropland patch sizes. More research is needed to explore the approaches to estimate fractional results for different crop types and crop patterns, especially in regions where patch sizes are smaller than the cell size of MODIS data.

Declarations of interest

None.

Acknowledgements

This research is partially supported by the Zhejiang Agriculture and Forestry University's Research and Development Fund (2013FR052) and by Belmont Forum funds for support for Batistella, Silva, and Moran (NSF 1531086). Batistella and Silva thank the São Paulo Research Foundation (Fapesp 2014/50628-9 and 2015/25892-7). Dutra thanks CNPq for the support of fieldwork through grants #401528/2012-0 and #309135/2015-0. Sanches and Luiz thank CNPq for the support of fieldwork through grant #402597/2012-5. The authors would like to thank the Center for Global Change and Earth Observations, Michigan State University for providing research support and facilities to Lu and Moran. We also want to thank the editor and anonymous reviewers for their valuable comments in improving this manuscript.

References

Arvor, D., Jonathan, M., Meirelles, M.S.P., Dubreuil, V., Durieux, L., 2011. Classification of MODIS EVI time series for crop mapping in the state of Mato Grosso, Brazil. Int. J. Remote Sens. 32, 7847–7871. http://dx.doi.org/10.1080/01431161.2010.531783.

Arvor, D., Dubreuil, V., Simões, M., Bégué, A., 2012. Mapping and spatial analysis of the soybean agricultural frontier in Mato Grosso, Brazil, using remote sensing data. GeoJournal 78, 833–850. http://dx.doi.org/10.1007/s10708-012-9469-3.
Breiman, L., 2001. Random forests. Mach. Learn. 45 (1), 5–32.
Brown, J.C., Jepson, W.E., Kastens, J.H., Wardlow, B.D., Lomas, J.M., Price, K.P., 2007. Multitemporal, moderate-spatial-resolution remote sensing of modern agricultural production and land modification in the Brazilian Amazon. GISci. Remote Sens. 44, 117–148. http://dx.doi.org/10.2747/1548-1603.44.2.117.
Brown, J.C., Kastens, J.H., Coutinho, A.C., Victoria, D.D.C., Bishop, C.R., 2013. Classifying multiyear agricultural land use data from Mato Grosso using time-series MODIS vegetation index data. Remote Sens. Environ. 130, 39–50. http://dx.doi.org/10.1016/j.rse.2012.11.009.
Chander, G., Markham, B.L., Helder, D.L., 2009. Summary of current radiometric calibration coefficients for Landsat MSS, TM, ETM+, and EO-1 ALI sensors. Remote Sens. Environ. 113, 893–903. http://dx.doi.org/10.1016/j.rse.2009.01.007.
Chang, J., Hansen, M.C., Pittman, K., Carroll, M., DiMiceli, C., 2007. Corn and soybean mapping in the United States using MODIS time-series data sets. Agron. J. 99, 1654–1664. http://dx.doi.org/10.2134/agronj2007.0170.
Chen, J., Jönsson, P., Tamura, M., Gu, Z., Matsushita, B., Eklundh, L., 2004. A simple method for reconstructing a high-quality NDVI time-series data set based on the Savitzky-Golay filter. Remote Sens. Environ. 91, 332–344. http://dx.doi.org/10.1016/j.rse.2004.03.014.
Chen, Y., Lu, D., Luo, G., Huang, J., 2015. Detection of vegetation abundance change in the alpine tree line using multitemporal Landsat Thematic Mapper imagery. Int. J. Remote Sens. 36, 4683–4701. http://dx.doi.org/10.1080/01431161.2015.1088675.
Chen, Y., Song, X., Wang, S., Huang, J., Mansaray, L.R., 2016. Impacts of spatial heterogeneity on crop area mapping in Canada using MODIS data. ISPRS J. Photogramm. Remote Sens. 119, 451–461. http://dx.doi.org/10.1016/j.isprsjprs.2016.07.007.
Cohn, A.S., Gil, J., Berger, T., Pellegrina, H., Toledo, C., 2016. Patterns and processes of pasture to crop conversion in Brazil: evidence from Mato Grosso state. Land Use Policy 55, 108–120. http://dx.doi.org/10.1016/j.landusepol.2016.03.005.
Congalton, R.G., Green, K., 2008. Assessing the Accuracy of Remotely Sensed Data: Principles and Practices. CRC press.
Dheeravath, V., Thenkabail, P.S., Chandrakantha, G., Noojipady, P., Reddy, G.P.O., Biradar, C.M., Gumma, M.K., Velpuri, M., 2010. Irrigated areas of India derived using MODIS 500 m time series for the years 2001–2003. ISPRS J. Photogramm. Remote Sens. 65, 42–59. http://dx.doi.org/10.1016/j.isprsjprs.2009.08.004.
Dias, L.C.P., Pimenta, F.M., Santos, A.B., Costa, M.H., Ladle, R.J., 2016. Patterns of land use, extensification, and intensification of Brazilian agriculture. Global Change Biol. 22, 2887–2903. http://dx.doi.org/10.1111/gcb.13314.
Epiphanio, R.D.V., Formaggio, A.R., Rudorff, B.F.T., Maeda, E.E., Luiz, A.J.B., 2010. Estimating soybean crop areas using spectral-temporal surfaces derived from MODIS images in Mato Grosso, Brazil. Pesq. Agropec. Bras. 45, 72–80. http://dx.doi.org/10.1590/S0100-204X2010000100010.
FAO (Food and Agriculture Organization of the United Nations), 2015. FAOSTAT Statistical Database. Food and Agriculture Organization of the United Nations, Rome.
Foody, G.M., 2009. Classification accuracy comparison: hypothesis tests and the use of confidence intervals in evaluations of difference, equivalence and non-inferiority. Remote Sens. Environ. 113, 1658–1663. http://dx.doi.org/10.1016/j.rse.2009.03.014.
Galford, G.L., Mustard, J.F., Melillo, J., Gendrin, A., Cerri, C.C., Cerri, C.E.P., 2008. Wavelet analysis of MODIS time series to detect expansion and intensification of row-crop agriculture in Brazil. Remote Sens. Environ. 112, 576–587. http://dx.doi.org/10.1016/j.rse.2007.05.017.
Grzegozewski, D.M., Johann, J.A., Uribe-Opazo, M.A., Mercante, E., Coutinho, A.C., 2016. Mapping soya bean and corn crops in the State of Paraná, Brazil, using EVI images from the MODIS sensor. Int. J. Remote Sens. 37, 1257–1275. http://dx.doi.org/10.1080/01431161.2016.1148285.
Guan, X., Huang, C., Liu, G., Meng, X., Liu, Q., 2016. Mapping rice cropping systems in Vietnam using an NDVI-based time-series similarity measurement based on DTW distance. Remote Sens. 8, 19. http://dx.doi.org/10.3390/rs8010019.
Gumma, M.K., Thenkabail, P.S., Maunahan, A., Islam, S., Nelson, A., 2014. Mapping seasonal rice cropland extent and area in the high cropping intensity environment of Bangladesh using MODIS 500 m data for the year 2010. ISPRS J. Photogramm. Remote Sens. 91, 98–113. http://dx.doi.org/10.1016/j.isprsjprs.2014.02.007.
Gumma, M.K., Thenkabail, P.S., Teluguntla, P., Rao, M.N., Mohammed, I.A., Whitbread, A.M., 2016. Mapping rice-fallow cropland areas for short-season grain legumes intensification in South Asia using MODIS 250 m time-series data. Int. J. Digital Earth 9 (10), 981–1003. http://dx.doi.org/10.1080/17538947.2016.1168489.
Gusso, A., Arvor, D., Ricardo Ducati, J., Veronez, M.R., Da Silveira, L.G., 2014. Assessing the MODIS crop detection algorithm for soybean crop area mapping and expansion in the Mato Grosso state, Brazil. Sci. World J. 2014. http://dx.doi.org/10.1155/2014/863141.
Hao, P., Zhan, Y., Wang, L., Niu, Z., Shakir, M., 2015. Feature selection of time series MODIS data for early crop classification using random forest: a case study in kansas, USA. Remote Sens. 7, 5347. http://dx.doi.org/10.3390/rs70505347.
IBGE (Brazilian Institute of Geography and Statistics), 2015. Crop Statistics in Brazilian Institute of Geography and Statistics. SIDRA.
Jönsson, P., Eklundh, L., 2004. TIMESAT-a program for analyzing time-series of satellite sensor data. Comput. Geosci. 30, 833–845. http://dx.doi.org/10.1016/j.cageo.2004.05.006.
Kumar, U., Kerle, N., Ramachandra, T.V., 2008. Constrained linear spectral unmixing technique for regional land cover mapping using MODIS data. In: Elleithy, K. (Ed.), Innovations and Advanced Techniques in Systems, Computing Sciences and Software Engineering. Springer Netherlands, Dordrecht, pp. 416–423. http://dx.doi.org/10.1007/978-1-4020-8735-6_78.
Li, G., Lu, D., Moran, E., Sant'Anna, S.J.S., 2012. A comparative analysis of classification algorithms and multiple sensor data for land use/land cover classification in the Brazilian Amazon. J. Appl. Remote Sens. 6 (1), 061706. http://dx.doi.org/10.1117/1.JRS.6 061706.
Lobell, D.B., Asner, G.P., 2004. Cropland distributions from temporal unmixing of MODIS data. Remote Sens. Environ. 93, 412–422. http://dx.doi.org/10.1016/j.rse.2004.08.002.
Lu, D., Weng, Q., 2007. A survey of image classification methods and techniques for improving classification performance. Int. J. Remote Sens. 28, 823–870. http://dx.doi.org/10.1080/01431160600746456.
Lu, D., Mausel, P., Brondizio, E., Moran, E., 2002. Assessment of atmospheric correction methods for Landsat TM data applicable to Amazon basin LBA research. Int. J. Remote Sens. 23, 2651–2671. http://dx.doi.org/10.1080/01431160110109642.
Lu, D., Moran, E., Batistella, M., 2003. Linear mixture model applied to Amazonian vegetation classification. Remote Sens. Environ. 87, 456–469. http://dx.doi.org/10.1016/j.rse.2002.06.001.
Lu, D., Batistella, M., Li, G., Moran, E., Hetrick, S., Freitas, C., Dutra, L., Sant'Anna, S.J.S., 2012. Land use/cover classification in the Brazilian Amazon using satellite images. Braz. J. Agric. Res. 47, 1185–1208. http://dx.doi.org/10.1590/S0100-204X2012000900004.
Lu, D., Li, G., Moran, E., Kuang, W., 2014. A comparative analysis of approaches for successional vegetation classification in the Brazilian Amazon. GISci. Remote Sens. 51, 695–709. http://dx.doi.org/10.1080/15481603.2014.983338.
Lunetta, R.S., Shao, Y., Ediriwickrema, J., Lyon, J.G., 2010. Monitoring agricultural cropping patterns across the Laurentian Great Lakes Basin using MODIS-NDVI data. Int. J. Appl. Earth Obs. Geoinf. 12, 81–88. http://dx.doi.org/10.1016/j.jag.2009.11.005.
Massey, R., Sankey, T., Congalton, R., Yadav, K., Thenkabail, P., Ozdogan, M., Meador, A., 2017. MODIS phenology-derived, multi-year distribution of conterminous U.S. crop types. Remote Sens. Environ. 198, 490–503. http://dx.doi.org/10.1016/j.rse.2017.06.033.
Maxwell, S.K., Nuckols, J.R., Ward, M.H., Hoffer, R.M., 2004. An automated approach to mapping corn from Landsat imagery. Comput. Electron. Agric. 43, 43–54. http://dx.doi.org/10.1016/j.compag.2003.09.001.
Mishra, N., Haque, M.O., Leigh, L., Aaron, D., Helder, D., Markham, B., 2014. Radiometric cross calibration of Landsat 8 operational land imager (OLI) and Landsat 7 enhanced thematic mapper plus (ETM+). Remote Sens. 6, 12619–12638. http://dx.doi.org/10.3390/rs61212619.
Odenweller, J.B., 1984. Crop identification using Landsat temporal-spectral profiles. Remote Sens. Environ. 14, 39–54. http://dx.doi.org/10.1016/0034-4257(84)90006-3.
Ozdogan, M., 2010. The spatial distribution of crop types from MODIS data: temporal unmixing using independent component analysis. Remote Sens. Environ. 114, 1190–1204. http://dx.doi.org/10.1016/j.rse.2010.01.006.
Pan, Y., Li, L., Zhang, J., Liang, S., Zhu, X., Sulla-Menashe, D., 2012. Winter wheat area estimation from MODIS-EVI time series data using the crop proportion phenology index. Remote Sens. Environ. 119, 232–242. http://dx.doi.org/10.1016/j.rse.2011.10.011.
Rudorff, B.F.T., Aguiar, D.A., Silva, W.F., Sugawara, L.M., Adami, M., Moreira, M.A., 2010. Studies on the rapid expansion of sugarcane for ethanol production in São Paulo State (Brazil) using landsat data. Remote Sens. 2, 1057. http://dx.doi.org/10.3390/rs2041057.
Savitzky, A., Golay, M.J., 1964. Smoothing and differentiation of data by simplified least squares procedures. Anal. Chem. 36, 1627–1639.
Teluguntla, P., Thenkabail, P.S., Xiong, J., Gumma, M.K., Congalton, R.G., Oliphant, A., Poehnelt, J., Yadav, K., Rao, M., Massey, R., 2017. Spectral matching techniques (SMTs) and automated cropland classification algorithms (ACCAs) for mapping croplands of Australia using MODIS 250-m time-series (2000–2015) data. Int. J. Digital Earth. http://dx.doi.org/10.1080/17538947.2016.1267269.
Thenkabail, P.S., Velpuri, M., 2006. A global map of rainfed cropland areas at the end of last millennium using remote sensing and geospatial techniques. Proc. SPIE 11, 114–129. http://dx.doi.org/10.1117/12.713204.
Thenkabail, P.S., Wu, Z., 2012. An automated cropland classification algorithm (ACCA) for Tajikistan by combining Landsat, MODIS, and secondary data. Remote Sens. 4, 2890. http://dx.doi.org/10.3390/rs4102890.
Thenkabail, P.S., Schull, M., Turral, H., 2005. Ganges and Indus river basin land use/land cover (LULC) and irrigated area mapping using continuous streams of MODIS data. Remote Sens. Environ. 95, 317–341. http://dx.doi.org/10.1016/j.rse.2004.12.018.
Victoria, D.d.C., Paz, A.R.d., Coutinho, A.C., Brown, J.C., 2012. Cropland area estimates using MODIS-NDVI times series in the state of Mato Grosso, Brazil. Pesq. Agropec. Bras. 47, 1270–1278. http://dx.doi.org/10.1590/S0100-204X2012000900012.
Vieira, M.A., Formaggio, A.R., Rennó, C.D., Atzberger, C., Aguiar, D.A., Mello, M.P., 2012. Object based image analysis and data mining applied to a remotely sensed Landsat time-series to map sugarcane over large areas. Remote Sens. Environ. 123, 553–562. http://dx.doi.org/10.1016/j.rse.2012.04.011.
Vintrou, E., Desbrosse, A., Bégué, A., Traoré, S., Baron, C., Seen, D.L., 2012. Crop area mapping in West Africa using landscape stratification of MODIS time series and comparison with existing global land products. Int. J. Appl. Earth Obs. Geoinf. 14, 83–93. http://dx.doi.org/10.1016/j.jag.2011.06.010.
Vourlitis, G.L., Hayashi, M., de S Nogueira, J., Caseiro, F.T., Campelo, J.H., 2002. Seasonal variations in the evapotranspiration of a transitional tropical forest of Mato Grosso, Brazil. Water Resour. Res. 38. http://dx.doi.org/10.1029/2000WR000122.
Wang, W., Yao, X., Tian, Y., Liu, X., Ni, J., Cao, W., Zhu, Y., 2012. Estimating leaf nitrogen concentration with three-band vegetation indices in rice and wheat. Field Crops Res. 129, 90–98. http://dx.doi.org/10.1016/j.fcr.2012.01.014.

Wardlow, B.D., Egbert, S.L., 2008. Large-area crop mapping using time-series MODIS 250 m NDVI data: an assessment for the US central great plains. Remote Sens. Environ. 112, 1096–1116. http://dx.doi.org/10.1016/j.rse.2007.07.019.

Wardlow, B.D., Egbert, S.L., 2010. A comparison of MODIS 250-m EVI and NDVI data for crop mapping: a case study for southwest Kansas. Int. J. Remote Sens. 31, 805–830. http://dx.doi.org/10.1080/01431160902897858.

Wardlow, B.D., Egbert, S.L., Kastens, J.H., 2007. Analysis of time-series MODIS 250 m vegetation index data for crop classification in the US Central Great Plains. Remote Sens. Environ. 108, 290–310. http://dx.doi.org/10.1016/j.rse.2006.11.021.

Xiao, X., Boles, S., Liu, J., Zhuang, D., Frolking, S., Li, C., Salas, W., Moore Iii, B., 2005. Mapping paddy rice agriculture in southern China using multi-temporal MODIS images. Remote Sens. Environ. 95, 480–492. http://dx.doi.org/10.1016/j.rse.2004.12.009.

Xiong, J., Thenkabail, P., Gumma, M., Teluguntla, P., Poehnelt, J., Congalton, R., Thau, Yadav K., 2017. Automated cropland mapping of continental Africa using Google Earth Engine cloud computing. ISPRS J. Photogramm. Remote Sens. 126, 225–244. http://dx.doi.org/10.1016/j.isprsjprs.2017.01.019.

Xu, X., Conrad, C., Doktor, D., 2017. Optimising phenological metrics extraction for different crop types in Germany using the Moderate Resolution Imaging Spectrometer (MODIS). Remote Sens. 9, 254. http://dx.doi.org/10.3390/rs9030254.

Zhang, M., Zhou, Q., Chen, Z., Liu, J., Zhou, Y., Cai, C., 2008. Crop discrimination in Northern China with double cropping systems using Fourier analysis of time-series MODIS data. Int. J. Appl. Earth Obs. Geoinf. 10, 476–485. http://dx.doi.org/10.1016/j.jag.2007.11.002.

Zheng, B., Myint, S.W., Thenkabail, P.S., Aggarwal, R.M., 2015. A support vector machine to identify irrigated crop types using time-series Landsat NDVI data. Int. J. Appl. Earth Observ. Geoinf. 34, 103–112. http://dx.doi.org/10.1016/j.jag.2014.07.002.

Zhong, L., Gong, P., Biging, G.S., 2014. Efficient corn and soybean mapping with temporal extendability: a multi-year experiment using Landsat imagery. Remote Sens. Environ. 140, 1–13. http://dx.doi.org/10.1016/j.rse.2013.08.023.

Zhong, C., Wang, C., Wu, C., 2015. MODIS-based fractional crop mapping in the U.S. midwest with spatially constrained phenological mixture analysis. Remote Sens. 7, 512. http://dx.doi.org/10.3390/rs70100512.

Zhong, L., Yu, L., Li, X., Hu, L., Gong, P., 2016. Rapid corn and soybean mapping in US Corn Belt and neighboring areas. Sci. Rep. 6. http://dx.doi.org/10.1038/srep36240.

Zhu, C., Lu, D., Victoria, D., Dutra, L., 2016. Mapping fractional cropland distribution in Mato Grosso, Brazil using time series MODIS enhanced vegetation index and Landsat Thematic Mapper data. Remote Sens. 8, 22. http://dx.doi.org/10.3390/rs8010022.

Zhu, L., Radeloff, V.C., Ives, A.R., 2017. Improving the mapping of crop types in the Midwestern U.S. by fusing Landsat and MODIS satellite data. Int. J. Appl. Earth Obs. Geoinf. 58, 1–11. http://dx.doi.org/10.1016/j.jag.2017.01.012.